



Keratin Composites and its Applications: A Review

Mayakrishnan Gopiraman,*^a Kim Ick Soo^b

^aDepartment of Applied Bioscience, College of Life and Environmental Science, Konkuk University, 120 Neungdong-ro, Gwangjin-gu, Seoul (05029), South Korea.

^bNano Fusion Technology Research Group, Division of Frontier Fibers, Institute for Fiber Engineering (IFES), Interdisciplinary Cluster for Cutting Edge Research (ICCER), Shinshu University, Tokida 3-15-1, Ueda, Nagano Prefecture 386-8567, Japan.

*Corresponding author E-mail address: gopiraman@konkuk.ac.kr (Gopiraman)

ISSN: XXXX-XXXX



Publication details

Received: 08th September 2020

Revised: 05th November 2020

Accepted: 16th November 2020

Published: 01st December 2020

Abstract: Keratin protein is a versatile biopolymer having exceptional properties such as remarkable biocompatibility and biodegradability for various applications. Keratin possesses many distinct advantages over conventional biomolecules, due to its intrinsic cellular recognition, high sulfur content and propensity for self-assembly. Typically, keratin has been extracted from various biowaste sources including hair, fingernails, shells, horn, hooves, toenails, beaks, feathers and claws. So far, several methods for the extraction of keratin protein have been developed. The keratin proteins can be improved and modified in many forms such as gels, films, beads, nanoparticles, and microparticles. After modification, its uses in various industries such as pharmaceuticals, cosmetic, food science and green chemistry is exceptional. Particularly, in recent years, research on the production of keratin has greatly increased due to the abundance of potential applications. The research and development of keratin protein are still continues to expand. The most important driving forces for this development are the increasing demand of this cost-effective keratin material. Hence, in this review, we mainly focus on the applications of keratin nanocomposites. In addition, part of this review focuses on the preparation methodologies and characterization techniques of the extracted keratin and keratin-based nanocomposites.

Keywords: Biomass; Keratin composites; Textiles; Catalysis; Biomedical; Energy; Agricultural

1. Introduction

A broad category of insoluble proteins that associate as intermediate filaments (IFs), a cytoskeletal element with 8–10 nm diameter, were being referred to the term “keratin”.^[1] Fig. 1 diagram showing inter- and intra-molecular bonding in keratin. Various chemical bonds (e.g. hydrogen, ionic and disulfide bonds) which result in increased strength and stability of the protein, determine the structure of the keratin. Based on structure, function and regulation, keratin is categorized into two distinct groups namely hard and soft.^[2,3] Hard keratins form ordered arrays of intermediate filaments embedded in a matrix of cystine rich proteins and contribute to the tough structure of epidermal appendages. However, soft keratins often form loosely-packed bundles of cytoplasmic intermediate filaments and typically contain less sulphur.^[4,5] Keratin can be extracted from various biowaste such as hair, fingernails, shells, horn, hooves, toenails, beaks, feathers and claws.^[6-8] Fig. 2 shows the biowaste sources of keratin. The extracted keratin materials have been utilized for various applications such as catalysis, energy, biomedical and textile applications. In fact, biomass derived keratin structural morphology is highly unique and it is nearly impossible to mimic the structure.^[9] For instance, PbS nanocrystals were formed within the keratin rich human hair-matrix during blacking.^[10] They found that

the shape and distribution of nanoparticles are controllable. Walter et al.,^[11] utilized keratin rich human hair fiber as a reactor/medium for the controlled synthesis of fluorescent Ag nanoparticles. Not only for the nanoparticles carrier, the keratin was used for wide range of applications and it has an ability to replace an expensive

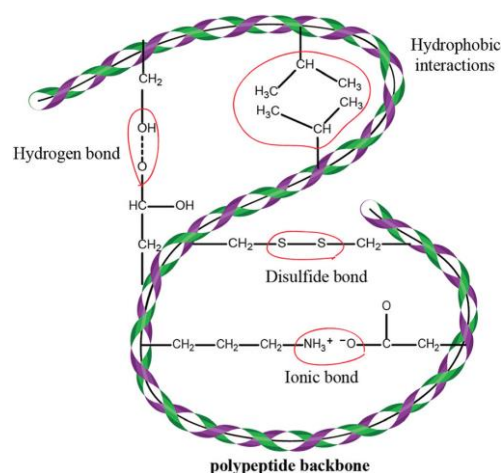


Fig. 1. Diagram showing inter- and intra-molecular bonding in keratin. Various chemical bonds, e.g. hydrogen, ionic and disulfide bonds, which result in increased strength and stability of the protein, determine the structure of the keratin.^[13]



Fig. 2. Biowaste sources of kertain.

2. Extraction methods of keratin from biomass

Keratin is a fibrous biological material, which represents a group of cysteine-rich filament-forming proteins.^[1-3] It can be found in nails, claws, beak, hair, wool, horns, and feathers.^[6-8,13] Based on their secondary structure, the keratin can be divided into two classes; α -keratin and β -keratin. Keratin is highly stable and it cannot be dissolved in both hot and cold water. Till date, keratin has been extracted from various biomass sources such as hair, fingernails, shells, horn, hooves, toenails, beaks, feathers and claws.^[13] In order to extract the keratin, so far several methods have been developed. The major methods used for the keratin extraction are reduction, oxidation, microwave irradiation, alkali extraction, steam explosion, sulfitolysis and ionic liquids. Keratin from the biomass (hair, fingernails, shells, horn, hooves, toenails, beaks, feathers and claws) is widely explored source for making valuable products. Some of the well-known methods are presented here. Fig. 3 shows the classification of various methods used for the extraction of keratin from keratin-rich materials, such as wool, feathers and hooves.

The structure of keratin is highly stable in both acidic and basic conditions mainly due to the disulfide bonds in the polypeptide chain.^[14] In order to extract the keratin, thiol containing chemicals are often used for the breaking the disulfide linkage.^[15,16] Extraction process requires very strong reducing agents.^[17] In addition, the processing conditions are also a key for the extraction of keratin. In the reduction method, most often used reagents are mercaptoethanol (MEC), thiourea, thioglycolic acid, urea, 2-mercaptoethanol and sodium dodecyl sulfate (SDS), Tris-HCl, EDTA, KCl-NaOH NaHCO₃, and DTT Tris.^[14-18] Several investigations examined the effects of various chemicals used in the reduction method. For the reduction of wool keratin, sodium thioglycolate and

biomaterials. Nanocellulose, wool-keratine, chitosan, natural pumice, mycelial, gram negative bacteria, and gram positive bacteria are some of the green materials reported to date.^[12] Keratin may be used instead of the above mentions biomaterials due to its cost-effectiveness. In spite of these advantages and availability, the biomass derived keratin is less investigated for its potential applications. However, particularly, in recent years, research on the production of keratin has greatly increased due to the abundance of potential applications. The research and development of keratin protein are still continues to expand. The most important driving forces for this development are the increasing demand of this cost-effective keratin material. Hence, in this review, we mainly focus on the preparation methodologies of keratin nanoparticles and its usefulness. In addition, part of this review focuses on the fabrication methods and applications of keratin-based nanocomposites.

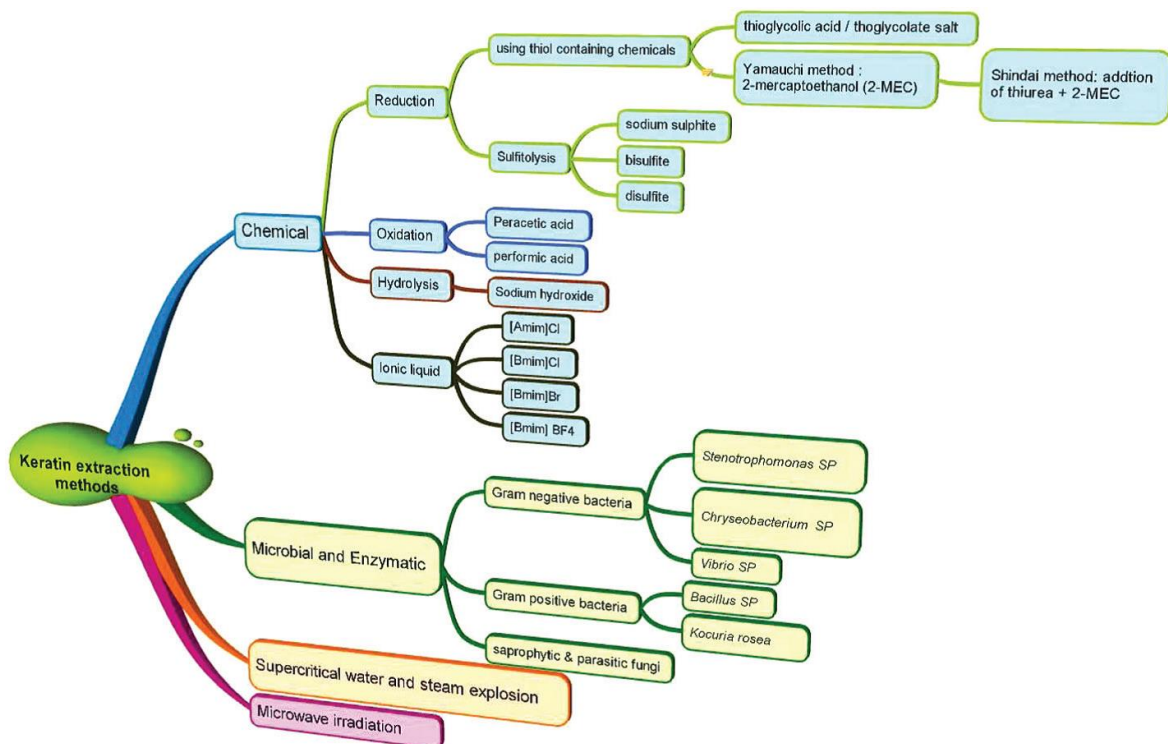


Fig. 3. Classification of various methods used for the extraction of keratin from keratin-rich materials, such as wool, feathers and hooves.^[13]

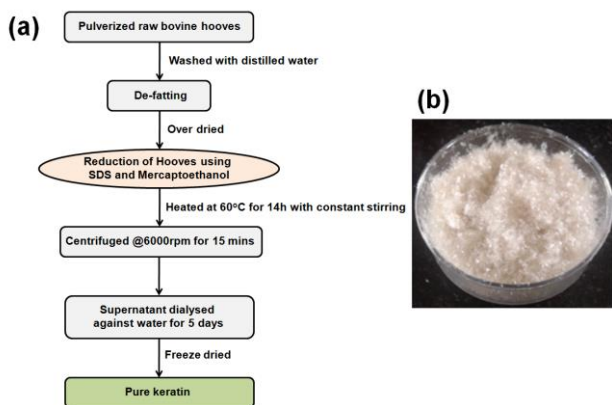


Fig. 4. Extraction of Hoof Keratin. (A) Flow chart describing the extraction procedure. (B) Lyophilized pure keratin.

thioglycolic acid, at different concentrations and pH values are studied. Goddard and co-workers^[19] concluded that wool can only be reduced at a pH of 10.5 or higher and no dissolution was observed at acidic or neutral pH. However, Savige and co-workers^[20] later reported considerable protein extraction at pH 2 using thiols at a moderate processing temperature (50–60°C). Although the bonding behaviour of the surfactant to keratin is documented, due to their structural, tertiary and secondary structures, as well as the differences in the degree of cross-linking of disulfide bonds, the interaction can be quite complicated depending on the type of keratin source, e.g. hair, wool, nail, hooves. Kitahara et al.^[21] extracted the epidermal types of keratins (such as skin differentiation keratin) by using 0.5 M 2-mercaptoethanol, whereas, hair types of keratins was extracted by increasing the thiol concentration to 2 M. Nakamura et al.^[35] reported a modified method of Yamauchi's method by combining thiourea and urea with MEC as reducing agents. The modified method is known as the "Shindai method" because it was developed at Shinshu University. Combination of thiourea and urea with MEC can work for the removal of proteins from the cortex more effectively compared to the conventional (developed by Yamauchi et al.^[22]), reported by Nakamura et al.^[23] They concluded that the Shindai method is better than the Yamauchi method^[22] in term of the keratin yield. Keratins with a high (110–135 kDa), medium (40–60 kDa) and low molecular weight of 10–20 kDa, can be reached by the Shindai method whilst the Yamauchi method resulted in proteins with a molecular mass of only 40–60 kDa. Therefore, Nakamura et al.^[23] suggested the addition of thiourea to improve the dissociation of the keratin proteins.

Kakkar et al.,^[24] extracted keratin from bovine hoof and it was used as a potential material for biomedical applications. Pulverized raw hooves were obtained from the local slaughter house at Perambur, Chennai (India). This material was washed thrice with distilled water to remove all dirt and then drained. After drying it completely in an oven, it was used as raw material for further studies. At first step, Soxhlet's apparatus was used to carry out defatting/delipidization of pulverized hoof sample for about two days using the mixture of hexane and dichloromethane. In the second step, a particular amount of hoof sample was mixed with enough amount urea, SDS and 2-mercaptoethanol in a round bottom flask and kept in orbital shaker at 60°C for 12 h to extract keratin at pH 7. The extracted keratin solution was then centrifuged and the supernatant was dialyzed against degassed water for several days. Some of the extracted keratin was kept in a deep freezer at –80°C for several hours and lyophilized to make it into powder. Fig. 4 shows the extraction of hoof keratin.

Kim et al.^[12,25-27] reported the extraction of keratin from human hair fibers. Human hair is a complex tissue that consists of proteins, lipids, water and pigments in which proteins of hard fibrous type known as keratin are largely present (67–88%). Although the human hair has advantages and availability, it has is often considered as biowaste. The human hair contains heteroatom (O, N and S) rich condensation polymers of amino acid. The cortex part is consists of cystine group (–s–s– bonds). The authors adopted Shindai method to extract the keratin from human hair. Initially, human hair powder was obtained from raw human hair by ball milling process. After washing well with distilled water and ethanol, the human hair powder stirred in a mixture of chloroform/methanol (2:1, v/v) for 3 days at 50°C to remove the lipids and dyes present in the human hair powder. Finally, the powder was mixed with a solution containing Tris–HCl (pH 8.5), thiourea, urea and 2-mercaptoethanol at 50°C for 24 h. The mixture was centrifuged and the keratin was dried. The resultant powder was used as catalyst support.

Keratin, the major protein in poultry feathers, hairs, and horns of animals, was water-stable and biocompatible and could be a promising biomaterial for medical applications. Xu et al.,^[28] reported intrinsically water-stable keratin nanoparticles for biomedical applications. In a typical extraction protocol of keratin, chicken feathers were washed well with ethanol and water in order to remove the lipid, water-soluble impurities and other impurities. For the purpose, chicken feathers were refluxed in ethanol using a Soxhlet extractor for 12 h. Hydrolysis was carried out for the cleaned

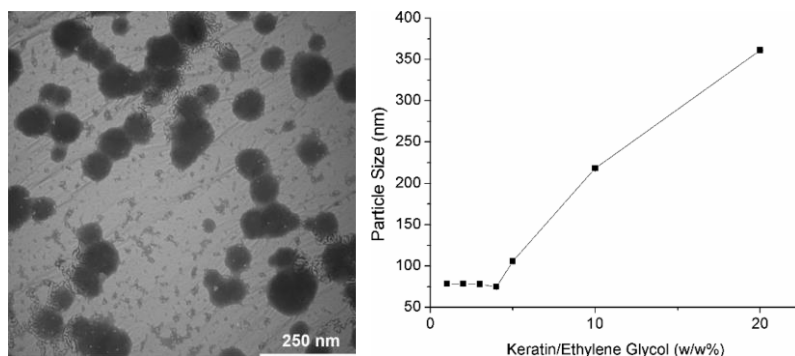


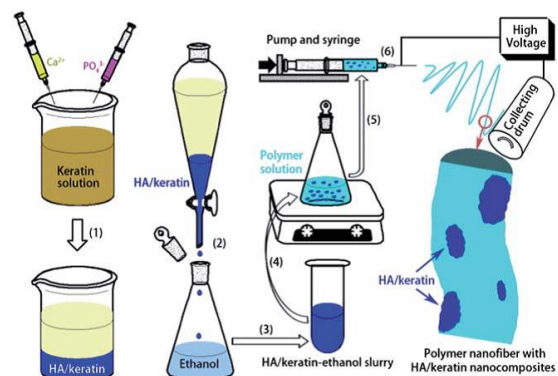
Fig. 5. Morphologies of keratin nanoparticles in a TEM image showing the diameters from 50 to 130 nm ((left)) and solid structures and (b) effect of keratin/ethylene glycol ratio on the particle sizes of keratin nanoparticles ((right)).^[28]

chicken feathers using 0.1 M sodium hydroxide at a ratio of 15:1 with sodium bisulfite (30% on weight of feathers) for 2 h at 80°C. Hydrochloric acid was added to precipitate hydrolyzed feather keratin. The dispersion was centrifuged and subsequently, the obtained precipitated keratin was washed using distilled water 3 times. The dried feather keratin was then pulverized into powder. To further, ethylene glycol with a weight ratio of keratin/water at 1:500 was used to convert the keratin powder into keratin nanoparticles under room temperature. To further break the keratin microparticles into nanoparticles, ultrasonication was applied. Finally, the dispersion of keratin nanoparticles were dialyzed (molecular weight cutoff of 7000) against distilled water for 4 days to remove ethylene glycol. The concentration of the keratin nanoparticles was adjusted via evaporation under reduced pressure. Fig. 5 shows the TEM morphologies of keratin nanoparticles showing the diameters from 50 to 130 nm and solid structures and the effect of keratin/ethylene glycol ratio on the particle sizes of keratin nanoparticles. The particle sizes varied from around 50 to 130 nm. The data showed that keratin concentration increased from 1 to 5% and then increased significantly from less than 100 nm to larger than 350 nm.

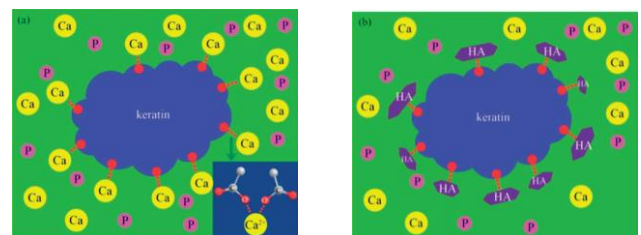
3. Synthesis of keratin nanocomposites

Numbers of nanomaterials is used for the preparation of nanocomposites. Namely, graphene, carbon nanotubes, silica, metal/metal oxide, carbon, polymers, and so on.^[29,30] The nanocomposites are proven to better when compare to raw materials. The key points are the dispersion and interaction between the materials which are selected for the preparation of composites. Nanocomposites are played crucial role in wide range of potential applications.^[31] Carbon-metal nanocomposites such as Ru/C and Cu/C,^[32] RGO/Au nanocomposite,^[33] graphene-Ru,^[34] RuO₂/SWCNT,^[35] Rh-nanoparticles/onion-like fullerene,^[36] NiO/SLG,^[37] and so on, are reported for potential various applications. Similarly, metal-metal oxide nanocomposites are also developed. For example, Raja et al.,^[38] prepared various transition metals (Cr, Mn, Fe and Co) substituted cerium site in CeVO₄ nanocomposite for oxidative dehydrogenation of 1-butene. Recently, polymer nanocomposites are played tremendous role in sensor, environmental, catalytic and biomedical applications.^[39-41] Ramkumar and co-workers^[42] obtained alumina-polymer nanocomposite for the removal of heavy metal ions from environmental samples. Keratin is also used to composite with metal nanoparticles, carbon nanomaterials and other support materials.

Biomimetic and bioactive inorganic-organic composite was prepared by using keratin and hydroxyapatite (HA) with sufficient electrospinnability.^[43] The chemical and physical structural intactness of HA and proteins in the polymer matrix were investigated to be excellent. The authors concluded that this type of scaffold can resemble the native extracellular matrix (ECM) as closely as possible and can induce cells to function naturally. Scheme 1 shows the well-known in situ biomimetic approach for the preparation of HA-keratin nanocomposites and the resultant nanocomposite was converted into nanofibers via the electrospinning process. The preparation process involves six steps; (1) HA-keratin nanocomposites were synthesized by adding calcium and phosphate ions into a keratin



Scheme 1. A schematic of the strategy to introduce HA-keratin nanocomposites into polymer nanofibers by the electrospinning process.^[43]



Scheme 2. Schematic illustration of the proposed mechanism for the generation of HA-keratin nanocomposites (not drawn to scale).^[43]

solution; (2) HA-keratin was dispersed and washed by ethanol several times to replace water completely; (3) the HA-keratin-ethanol slurry was collected by centrifugation; (4) HA-keratin-ethanol was dispersed into the polymer solution homogeneously; (5) and (6) polymer solution was electrospun into polymer nanofibers with HA-keratin nanocomposites.

Scheme 2 shows the schematic illustration of the proposed mechanism for the generation of HA-keratin nanocomposites. The presence of large amount of active groups, such as carboxyl or carbonyl groups, keratin could chelate the calcium ions, which act as efficient nucleation sites for HA nanocrystals. In general, the growth of the mineral phase can be controlled by long collagen fibril, whereas, the irregular keratin fractions could not control the growth direction of HA crystals. Interestingly, the formation of big crystals can be stopped due to the retarded supply of calcium ions from the solution to the HA nuclei. In fact, most of the calcium ions were captured by the carboxyl and carbonyl groups of the keratin chains.

Graphene has been discovered as a “rising-star” nanomaterial and has attracted huge attention due to unique physicochemical properties such as chemical inertness, thermal stability and a huge surface area. Recently graphene has been used for the preparation of various nanocomposites. For example, mechanically strong cellulose acetate/graphene hybrid nanofibers were prepared by Kim and co-workers. Fujimori et al.,^[44] prepared poly(vinyl alcohol) (PVA)/graphene and PVA/multi-walled carbon nanotube (MWCNT) composite nanofibers via simple electrospinning technique. The nanocomposites showed good mechanical strength and electromagnetic interference shielding effectiveness (EMI SE). Keratin/graphene composite was prepared by Rodriguez-Gonzalez et al.^[45] The fibrous membrane was used for bone tissue engineering.

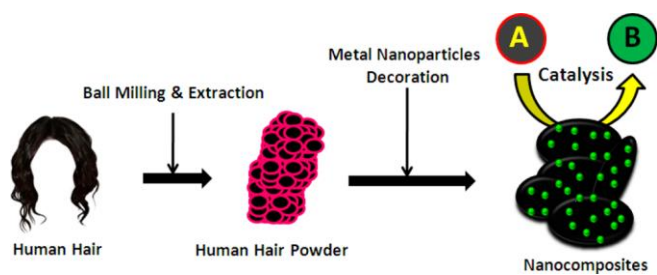


Fig. 6. Schematic illustration of the preparation of MNPs/e-HHP.^[27]

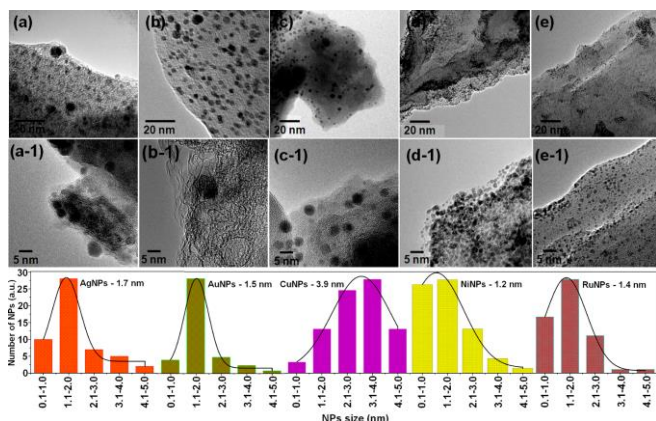


Fig. 7. HRTEM images of (a, a-1) AgNPs/e-HHP, (b, b-1) AuNPs/e-HHP, (c, c-1) CuNPs/e-HHP, (d, d-1) NiNPs/e-HHP, and (e, e-1) RuNPs/e-HHP. Bottom panel: histogram showing particle size distribution of MNPs; calculated using Image J.^[27]

The typical procedure as follows; keratin (obtained from the biofiber of chicken feathers in salt form) were dissolved in a mixture of distilled water, urea, EDTA, and 2-mercaptoethanol with vigorous stirring for 24 h at room temperature. The keratin salt then is dialyzed for three days. On other hand, graphite oxide-water dispersion was prepared using ultrasonic bath. The grafting reaction is performed under a redox system by mixing the dispersion of GO sheets with dialyzed keratin, H_2SO_4 , malic acid, and $KMnO_4$ at $65^\circ C$ for 3 h. The morphology and thickness of keratin-grafted graphene oxide (GKGO) sheets were investigated by TEM and AFM.

Kim et al., utilized the human hair (HH) for the preparation of keratin nanocomposites^[12,25-27]. They found that the human hair is a highly suitable platform for the decoration of various metal nanoparticles (NPs). Briefly, a fine human hair powder (HHP) was obtained by a simple ball milling of raw human hair. Then the easily leachable constituents such as lipids and dyes present in the fine human hair powder were removed after stirring with a mixture of chloroform/methanol at elevated temperatures. The obtained HHP was treated with a mixture of Tris-HCl, thiourea, urea and 2-mercaptoethanol to obtain keratin. The resultant keratin (e-HHP) was used as a suitable platform for the decoration of metal NPs. In a typical method for the decoration of metal NPs on human hair derived keratin, the e-HHP was dispersed in aqueous solution containing metal salts ($AgNO_3$, $CuCl_2 \cdot 2H_2O$, $NiCl_2 \cdot 6H_2O$, $HAuCl_3 \cdot xH_2O$ or $RuCl_3$) and the mixture was stirred at elevated temperatures to enhance the interaction between the metal ions and ONS donor groups of human hair derived keratin. Subsequently, the metal salts were reduced to metallic nanoparticles (Ag, Au, Ni, Ru or

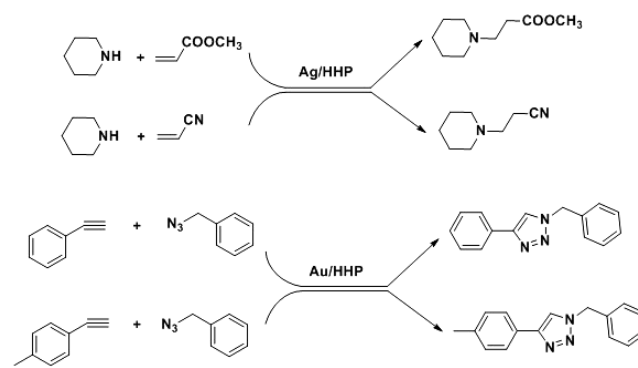
Cu NPs) by a dropwise addition of aqueous $NaBH_4$ solution. Finally, the keratin nanocomposites (AgNPs/e-HHP, AuNPs/e-HHP, CuNPs/e-HHP, NiNPs/e-HHP, and RuNPs/e-HHP) were filtered out and vacuum dried.^[27] Fig. 6 shows the schematic illustration for the preparation of metal nanoparticles supported keratin nanocomposites. They found that the metal NPs are accurate spherical in shape and the mean diameters of metal NPs are very small (typically under 5 nm). In addition, strong attachment between metal NPs and human hair derived keratin was confirmed by various spectroscopic and microscopic techniques. In fact the electron donor groups (S, N, and O) present in the human hair derived keratin assisted the formation of such small metal NPs on e-HHP with very strong attachment. Fig. 6 shows the HRTEM images of keratin nanocomposites and histogram showing particle size distribution of metal NPs.

4. Applications of keratin and its nanocomposites

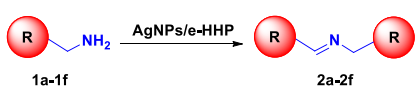
Biomass derived keratin nanocomposites have been demonstrated valuable candidate in various potential applications such as catalysis, energy and biomedical. In order to achieve best results, the form of keratin is modified. For example, keratin requires high temperature carbonization for obtaining high quality electrode materials for energy applications. Similarly, nano form of the keratin is often used for the catalysis applications. There are several reports studied such types of work.

4.1. Catalytic applications

Alike common supports (such as silica, alumina, carbon materials, polymers and metal oxides), keratin is also efficiently used as support for the active nanoparticles catalysts.^[46,47] In generally, the keratin not only provides better metal-support interaction but also physicochemical stable and insoluble in most of the organic solvents due to the presence of strong S-S bonds between cysteine molecules.^[25] Hence, very recently, keratin nanocomposites have been demonstrated as an efficient heterogeneous nanocatalyst for various organic transformations. Kim and research group^[12,25-27] demonstrated various catalytic reaction by using keratin supported transition metal nanocatalysts. It was found that the human hair is highly suitable platform for the active metal nanoparticles such as Ag, Au, Ni, Cu, Pd and Ru. Deng et al.,^[12] developed Ag/HHP and Au/HHP nanocatalysts and efficiently utilized for cyclo addition

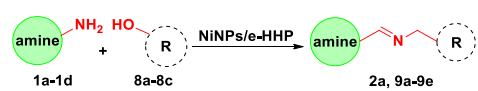


Scheme 3. Ag/HHP catalyzed aza-Michael and Au/HHP catalyzed [3+2] cycloaddition reaction.

Table 1. AgNPs/e-HHP catalyzed self-coupling of amines to imines^{a [27]}


Product	Yield (%)	Time (h)	TON/TOF
2a	85 ^b , (85) ^c , 79% ^d , 100% ^e	24 h	(93/4 h ⁻¹) ^f
2b	29% ^b , (29%) ^c , 100% ^e	24 h	(32/1 h ⁻¹) ^f
2c	92% ^b , (92%) ^c , 81% ^d , 100% ^e	16 h	(101/6 h ⁻¹) ^f
2d	99% ^b , (99%) ^c , 81% ^d , 100% ^e	24 h	(108/5 h ⁻¹) ^f
1e	40% ^b	4 h	
1f	36% ^b	24 h	

^aReaction conditions: 109.2 μL of benzylamine (1 mmol), 25 mg of AgNPs/e-HHP (0.91 mol% of Ag), 110°C, under air atmosphere. ^bGC conversion. ^cGC yield. ^dIsolated yield. ^eSelectivity. ^fTON/TOF.

Table 2. NiNPs/e-HHP catalyzed one pot synthesis of imines from the coupling of alcohols and primary amines^{a [27]}


Product	Yield (%)	Time (h)	TON/TOF
2a	83% ^b , 83% ^c , 79% ^d , 100% ^e	24 h	(69/3 h ⁻¹) ^f
9a	92% ^b , 92% ^c , 87% ^d , 100% ^e	24 h	(77/3 h ⁻¹) ^f
9b	79% ^b , 9% ^c , 30% ^e	40 h	(8/0.2 h ⁻¹) ^f
9c	36% ^b , 24% ^c , 88% ^e	40 h	(20/0.5 h ⁻¹) ^f
9d	83% ^b , 83% ^c , 75% ^d , 100% ^e	17 h	(69/4 h ⁻¹) ^f
9e	13% ^b , 13% ^c , 100% ^e	24 h	(11/0.5 h ⁻¹) ^f

^aReaction conditions: amine (1.2 mmol), alcohol (1 mmol), NiNPs/e-HHP (1.2 mol % of Ni), toluene (3 ml), 110°C, under N₂ atmosphere. ^bGC conversion. ^cGC yield. ^dIsolated yield. ^eSelectivity. ^fTON/TOF.

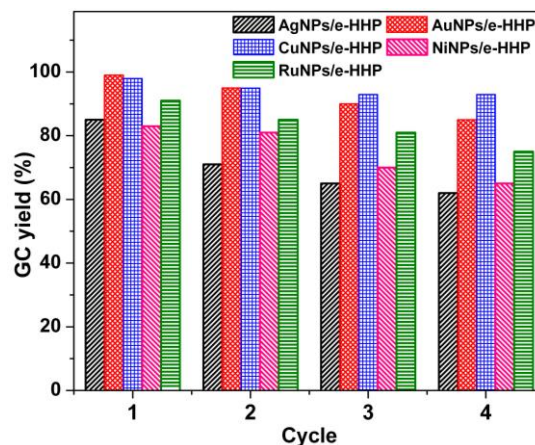
and aza-Michael reactions, respectively. The reusability and heterogeneity tests of the nanocatalysts were also found to be excellent. Under optimized conditions, Ag/HHP gave methyl 3-(piperidin-1-yl) propanoate in excellent yield (>99%) with 100% selectivity from the reaction of piperidine and methyl acrylate (Scheme 3). The system showed high TON/TOF value of 619/2475 h⁻¹. Similarly, a better 91% yield of 1-benzyl-4-phenyl-1H-1,2,3-triazole with excellent TON/TOF (433/217 h⁻¹) was obtained from Au/HHP-mediated cycloaddition of ethynylbenzene and (azidomethyl)benzene (Scheme 3). The results showed that the catalysts are not only active but also selective and reusable.

Zero-valent state of metal nanoparticles (Ag, Au, Cu, Ni and Ru) was supported on human hair with a very strong metal-support interaction. The obtained AgNPs/e-HHP, AuNPs/e-HHP, CuNPs/e-HHP, NiNPs/e-HHP, and RuNPs/e-HHP catalysts were employed for the self-coupling of amines, N-oxidation of tertiary amines, aza-Michael reaction, imines synthesis, and oxidation of alcohols, respectively.^[27] They proved that the loading of metal on e-HHP can be easily controlled. Merit of these MNPs/e-HHP materials was recognized from the superior catalytic activity. Notably, by anchoring Ag and Ni nanoparticles on e-HHP, the inactive Ag and Ni nanoparticles were tuned out to be active systems for self-coupling of amines and one pot synthesis of imines, respectively. It is well known that most of the Ag-based catalysts are proved to be inefficient for the self-coupling of amines.^[48] Interestingly, the human hair supported Ag nanoparticles solved the drawback of Ag-based systems. The results confirm that a variety of imines were successfully obtained from the homocoupling of primary amines (Table 1). The reaction conditions as follows: benzylamine (1 mmol), 25 mg of AgNPs/e-HHP (0.91 mol% of Ag), 110°C, under air atmosphere. For example, the Ag-human hair catalyst gave N-benzylidene-1-phenylmethanamine (2a) by the transformation of benzylamine (1a) in good yield (85%) with 100% selectivity (Table 1, entry 2a). Similarly, to overcome the drawback of Ni-based heterogeneous systems in one-pot imine synthesis, NiNPs/e-HHP catalyst was used for the same.^[49] The optimized reaction condition is: amine (1.2 mmol), alcohol (1 mmol), NiNPs/e-HHP (1.2 mol % of Ni), toluene (3 ml), 110°C, under N₂ atmosphere. Surprisingly, under

Human hair support turned inactive Ni and Ag NPs to be an active catalyst for imine synthesis

the optimized conditions, coupling of 1a and benzyl alcohol gave 2a in 83% yield with 100% selectivity (Table 2, entry 2a). It was found that the fresh e-HHP is not suitable for the one-pot imine synthesis since it gave a trace amount of the desired product from the reaction between 1a and benzyl alcohol. Overall, the advantages and excellent catalytic activity of MNPs/e-HHP make HH as a preferable catalyst support.

Reusability of heterogeneous catalyst is one of the very important requirements. Fig. 8 shows the reusability of metal nanocomposites derived from human hair. The obtained AgNPs/e-HHP, AuNPs/e-HHP, CuNPs/e-HHP, NiNPs/e-HHP, and RuNPs/e-HHP catalysts can be reused for the self-coupling of amines, N-oxidation of tertiary amines, aza-Michael reaction, imines synthesis, and oxidation of alcohols, respectively; the catalysts showed good yield even after 4th cycles.^[27]

**Fig. 8.** Reusability of metal nanocomposites derived from human hair.^[27]

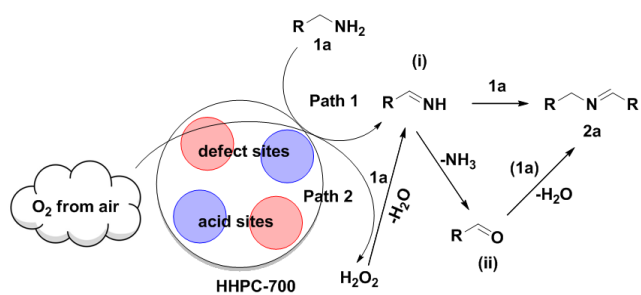


Fig. 9. Possible mechanism for self-coupling of benzylamine catalyzed by HHPC-700; 1a – benzylamine; 2a – (Z)-N-benzyl-1-phenylmethanimine.^[50]

Chung and co-workers^[50] transformed human hair to heteroatom-rich hierarchically porous carbon nanosheets (HPCN-700) by simple chemical activation process. Presence of heteroatoms (O, N and S) and oxygen functional groups in HPCN-700 was confirmed. The HPCN-700 demonstrated as a catalyst for the homocoupling of amines to imines. The results reflect that the catalytic system could access a wide range of amines could be actively transformed to corresponding imines with excellent yield and selectivity. Interestingly, the catalyst can be easily recovered and reused for several cycles. The mechanism proved that the activity of catalyst is mainly due to the presence of heteroatom (active sites). This is the main advantage of the heteroatom rich human hair transforming into defective activated carbon. Fig. 9 shows the possible mechanism for self-coupling of benzylamine catalyzed by HHPC-700. Two different routes, path 1 and 2, have been proposed. In path 1, benzylamine gets activated by defect sites of HHPC-700 to form RCH=NH as an intermediate and it further reacts with another amine to form imine after losing NH₃. In path 2, HHPC-700 accesses both O₂ (from air) and amine to form H₂O₂ and RCH=NH as intermediates. Subsequently, the RCH=NH loses NH₃ to form aldehyde which then reacts with benzylamine to give self-coupled product imine by losing water. It is worth mentioning that most of the activated carbon catalyst showed poor reusability in the homocoupling of amines to imines. However, the HHPC-700 can be reused at least for 3 cycles. The HHPC-700 affords 81 and 75 % of 2a at 2nd and 3rd cycles respectively. The catalyst is cost-effective and environmentally viable.

Use of aminophenol and its derivatives is well known in various potential applications. They are used as corrosion inhibitor, analgesic and antipyretic drugs, photographic developer and anticorrosion-lubricant.^[51] In particular, 2- and 4-aminophenol is widely used in the various industrial applications such as pharmaceuticals and fine chemicals. Although several methods are available for obtaining 2- and 4-aminophenol, the catalytic reduction method is the simple and cost effective process for the preparation of aminophenols. The U.S. Environmental Protection Agency listed the nitrophenols as the most common organic pollutants could be found in agricultural and industrial wastewaters.^[52] In addition, due to the carcinogenesis, hepatotoxicity and mutagenesis of the nitrophenols, they have been listed in the "Priority Pollutions List" by U.S. Environmental Protection Agency.^[53] Traditional processes such as electrochemical treatment, microwave-assisted catalytic oxidation, electro coagulation, microbial degradation and adsorption to treat the organic pollutants are highly limited. Recent days, the catalytic

process of such organic pollutants to valuable compounds is highly focused. In addition, the catalytic processes are straightforward and environmentally feasible approach.

Well known catalytic transition metals supported catalysts based on Ag, Au, Ni, Cu, Pd, Pt, Ru, Fe and Mn are best proven towards the reduction of 4-nitrophenol. Some of the highly efficient catalysts reported heterogeneous catalysts for the reduction of 4-nitrophenol are Cu/Fe₃O₄ nanoparticles, 1T-MoS₂/RGO nanocomposite, porous Au@Pd@RuNPs, Ag-x/C (Ag-1/C, Ag-2/C and Ag-3/C), porous Au@PdNPs, CNT-AuNP-anti-AFP and AuNP-anti-AFP, Pt-Au-pNDs/RGOs, bimetallic alloys (Pt/Cu, Pd/Cu, Pd/Au, Pt/Au, and Au/Cu DENs), Ag/TiO₂ nanocomposites, RuDEN, G-Ni₃₀Pd₇₀, Au/PMMA, Ni@Pd core-shell nanoparticles, Ni-RGO, Ni/MC-750 and Ag-Au-rGO nanocomposites.^[54-63] Interestingly, Gopiraman et al.,^[12,25-27] proved that the human hair powder can also be used as catalyst support for incorporating catalytic active materials for the treatment of organic pollutants in water. Several transition metals such as Ag, Au, Ni, Cu, and Ru supported catalysts prepared for catalytic applications. It was concluded that human hair nanocomposites (Ag/HHP and Ru/HHP) would also be a better choice for the catalytic reduction of 4-nitrophenol to 4-aminophenol. Excellent catalytic activity of Ag/HHP and Ru/HHP towards the reduction of 4-NP was confirmed by Kim and group.^[25] They found that the human hair nanocomposites are not only active but also highly reusable and stable. Fig. 10 shows UV-vis spectra of the reduction of 4-nitrophenol in aqueous solution recorded every 1 min using different amount of Ru/HHP and the plots of ln[C_t/C₀] versus reaction time for the reduction of 4-nitrophenol with NaBH₄ over e-HHP, Ag/HHP and Ru/HHP. The Ag/HHP and Ru/HHP showed very high rate constant (k_{app}) values of 5.94 × 10⁻² s⁻¹ (by Ag/HHP) and 6.12 × 10⁻² s⁻¹ (by Ru/HHP) for the reduction of 4-nitrophenol. Notably, the Ag/HHP and Ru/HHP can be reused without significant loss in its catalytic activity (Fig. 11a). Physicochemical stability of Ag/HHP and Ru/HHP (after 10th use) was also found to be excellent. Moreover, the results confirmed that the Ag/HHP and Ru/HHP catalysts are highly stable. Mechanism was also proposed for the Ag/HHP and Ru/HHP catalyzed reduction of 4-nitrophenol. Fig. 11b shows the proposed mechanism for the Ag/HHP and Ru/HHP mediated reduction reaction of 4-nitrophenol. In the reduction process, BH₄⁻ and nitro groups act as donor and acceptor groups respectively. During the process, metal nanoparticles acts as an electronic relay system and accelerates the electron transfer from BH₄⁻ to nitro groups and the system subsequently gives 4-aminophenol.

4.2. Energy Applications

Energy storage is gaining importance in both conventional and renewable energy sector worldwide.^[69,70] In the renewable energy sector the energy storage systems show huge potential due to several applications and benefits. For this purpose, active electrode materials are prepared using several source materials. Among them, biomass derived activated carbon reorganized to be the cheap and efficient. For example, biomass materials, namely, corn fibers (CF), corn leaves (CL), and corn cobs (CC) were utilized to transform the materials into exciting two-dimensional (2D) and three-dimensional (3D) carbon nanoarchitectures (HPCNs) with excellent physicochemical properties.^[71] The HPCNs demonstrated huge BET

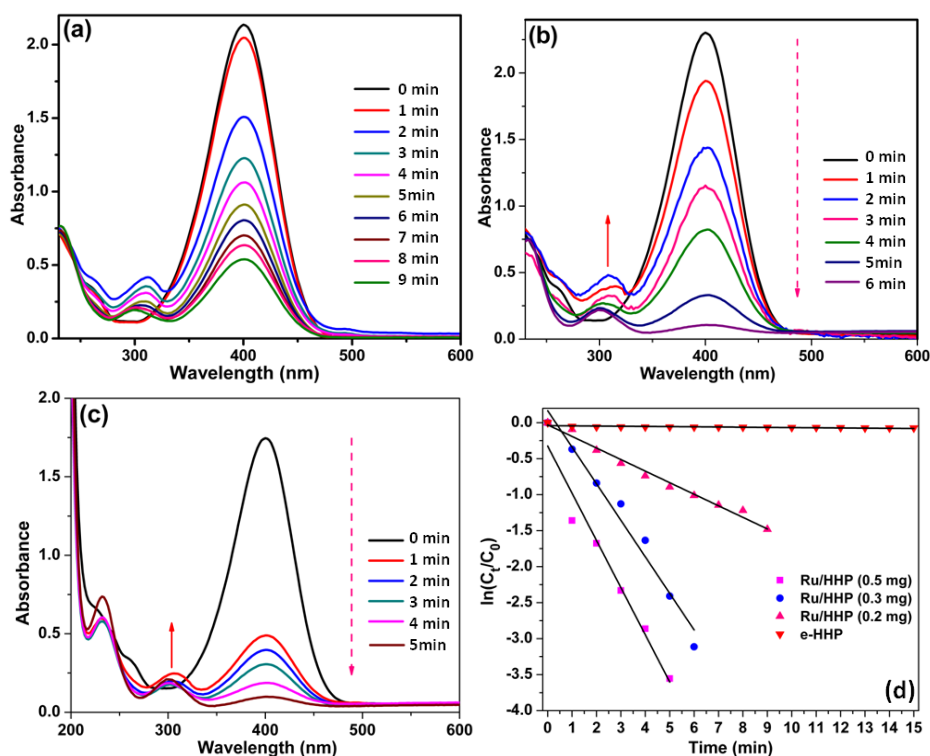


Fig. 10. UV-vis spectra of the reduction of 4-NP in aqueous solution recorded every 1 min using different amount of Ru/HHP (a) 0.2 mg, (b) 0.3 mg and (c) 0.5 mg. (d) Plots of $\ln(C_t/C_0)$ versus reaction time for the reduction of 4-NP with NaBH_4 over e-HHP, Ag/HHP and Ru/HHP.^[25]

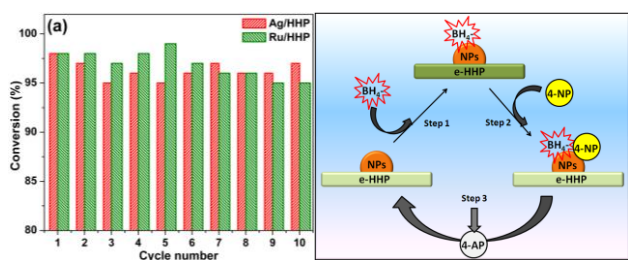


Fig. 11. (a) Reusability of Ag/HHP and Ru/HHP, and (b) proposed mechanism for the reduction of 4-NP by nanocomposites.^[25]

surface area of around 2394–3475 m^2/g . The HPCNs showed a maximum specific capacitance of 575 F/g in 1.0 M H_2SO_4 with good stability over 20,000 cycles. Similarly, keratin-rich biomass materials are utilized for the preparation of such activated carbon electrode materials. Qian et al.,^[72] utilized Chinese human hair fibers to obtain heteroatom doped porous carbon flakes and it was employed for high-performance supercapacitor electrode materials. Scheme 4 shows flow diagram for the fabrication of HMCs. They found that human hair carbonized at 800°C showed high charge storage capacity with a specific capacitance of 340 F g^{-1} in 6 M KOH at a current density of 1 A g^{-1} and good stability over 20000 cycles. Fig. 12 shows electrochemical performance characteristics measured in a three-electrode system in the 6 M KOH electrolyte.

Alike, the human hair derived needle like- MnO_2 nanostructure (MnO_2/ACs nanocomposites) was prepared and it was used as electrode material for supercapacitor. Interestingly, the MnO_2/ACs nanocomposites showed an excellent capacitance in three different electrolytes (1.0 M H_2SO_4 , 1.0 M KOH and 1.0 M Na_2SO_4). The MnO_2/ACs (1 : 12) achieved a maximum capacitance of 410 F g^{-1} , 345

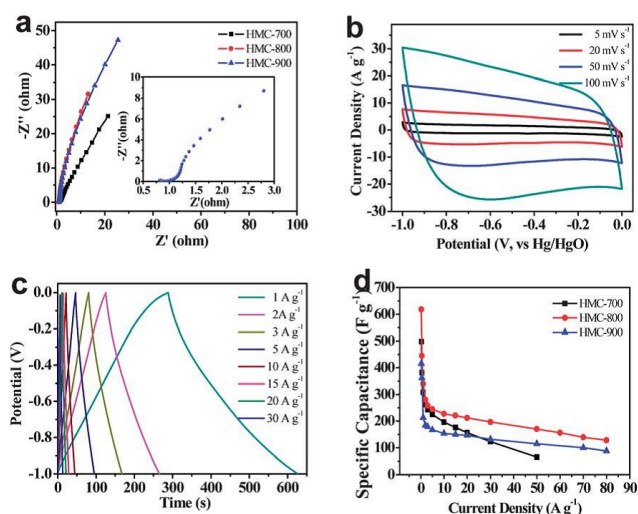


Fig. 12. Electrochemical performance characteristics measured in a three-electrode system in the 6 M KOH electrolyte. (a) Electrochemical impedance spectra (inset: magnified 0.5–3 Ω region) under the influence of an ac voltage of 5 mV. (b) Cyclic voltammograms of HMC-800 at different scan rates. (c) Charge–discharge curves of HMC-800 at different current densities. (d) Specific capacitances of HMC-700, HMC-800, HMC-900 at different current densities.



Scheme 4. Flow diagram for the fabrication of HMCs. Hair fibers are pre-carbonized at 300°C and then mixed with KOH (weight KOH : weight carbon $\frac{1}{2}$: 1) and further carbonized at 700, 800, and 900 °C, respectively.

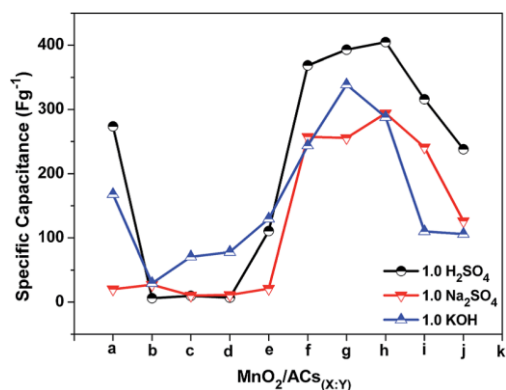


Fig. 13. Specific capacitances of (a) pure ACs, (b) $\text{MnO}_2/\text{ACs}(1 : 2)$, (c) $\text{MnO}_2/\text{ACs}(1 : 1)$, (d) $\text{MnO}_2/\text{ACs}(1 : 2)$, (e) $\text{MnO}_2/\text{ACs}(1 : 4)$, (f) $\text{MnO}_2/\text{ACs}(1 : 8)$, (g) $\text{MnO}_2/\text{ACs}(1 : 10)$, (h) $\text{MnO}_2/\text{ACs}(1 : 12)$, (i) $\text{MnO}_2/\text{ACs}(1 : 14)$, and (j) $\text{MnO}_2/\text{ACs}(1 : 16)$ at scan rate of 5 mV s^{-1} .

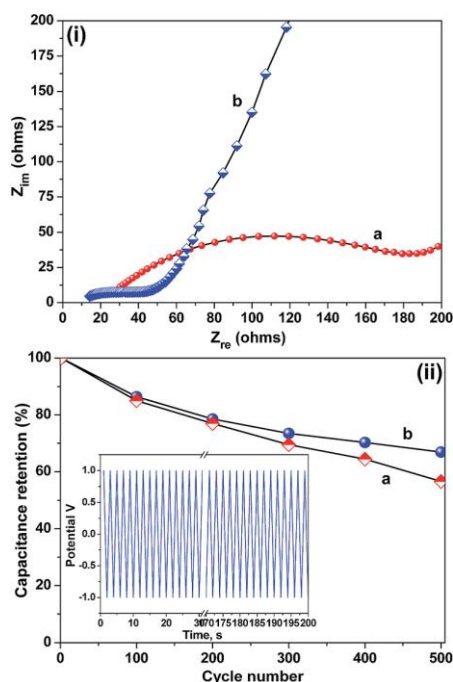


Fig. 14. (i) Nyquist plots of (a) pure ACs and $\text{MnO}_2/\text{ACs}(X:Y)$ recorded in $1.0 \text{ M H}_2\text{SO}_4$ and (ii) cycle stability of pure ACs (a) and $\text{MnO}_2/\text{ACs}(X:Y)$ (b) in $1.0 \text{ M H}_2\text{SO}_4$; inset: galvanostatic charge-discharge cycles.

F g^{-1} and 291 F g^{-1} in $1.0 \text{ M H}_2\text{SO}_4$, 1.0 KOH and $1.0 \text{ Na}_2\text{SO}_4$, respectively. Moreover, the $\text{MnO}_2/\text{ACs}(1 : 12)$ showed capacitance of 300 F g^{-1} even after 500 cycles in $1.0 \text{ M H}_2\text{SO}_4$. It was found that the better performance of the $\text{MnO}_2/\text{ACs}(X:Y)$ is due to five obvious reasons (i) the high specific surface area, (ii) high average pore size and mean pore volume, (iii) the presence of heteroatom such as O, S and N, (iv) conductivity of carbon and (v) needle-like MnO_2 . Fig. 13 shows specific capacitances of pure ACs, MnO_2/ACs with different AC: MnO_2 weight ratios at scan rate of 5 mV s^{-1} . Fig. 14a shows EIS spectra of ACs and $\text{MnO}_2/\text{ACs}(1:12)$ and the cycle stability of $\text{MnO}_2/\text{ACs}(1:12)$. A depressed semicircle and a smaller interfacial charge-transfer resistance, representing good conductivity of the materials and high ion transfer speed across interfaces between the electrolyte and electrode. Fig. 14b represents the cycle stability of pure ACs and $\text{MnO}_2/\text{ACs}(1:12)$ at scan rate of 5 mV s^{-1} in 1.0 M

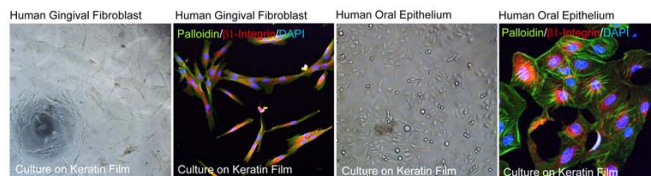


Fig. 15. Cell adhesion and 1 integrin expression on keratin substrate.

H_2SO_4 . It was calculated that about 70% of the Cs was maintained by the $\text{MnO}_2/\text{ACs}(1:12)$ after 500 cycles. In spite of the excellent results, there is no significant number of reports published on human hair-based energy storage systems.

4.3. Biomedical applications

To date, number of biomaterials including polymers,^[74] metal/metal oxide,^[75] bioceramics and naturally derived biomaterials are reported as an efficient candidate for the poetical applications in tissue engineering and regenerative medicine.^[76] In particular, collagen can be derived from naturally occurring biowaste materials and their use in clinical applications is highly commended. In fact, the naturally derived collagen possesses favorable biocompatibility, biological function, and biodegradability properties. Well-known clinical use of collagen is dermal filler, dental barrier membrane, dressing membrane and nerve conduit. Interestingly, keratin has molecular structures similar to collagen, the prominent protein in native extracellular matrices (ECMs). Furthermore, keratin-based materials can easily promote cell adhesion on its surface due to the presence of tripeptides “Arg-Gly-Asp” (RGD) and “Leu-Asp-Val” (LDV) in keratin molecules. Fig. 15 shows the cell adhesion and 1 integrin expression on keratin substrate. In generally, the keratin materials are highly stable in water because of the highly cross-linked molecular structures attributed to the 7% cysteine in the amino acid components. Hence, unlike other biomaterials, water stability of keratin highly favors for the biomedical applications. In addition, the intrinsic water stability of keratin is advantageous over other proteins as nanoparticles. Silver nanoparticles are found to be the most efficient bioactive material. Keratin is a suitable carrier for the bioactive silver nanoparticles. It is often achieved with polyethylene glycol grafting or using toxic solvent. Research on the development of a better method is underway, and the biodistribution should be investigated for drug delivery purposes.

Layer by layer assembly is one of the most often adopted methods for the preparation of the keratin biomaterials.^[77-80] Although many other physical and chemical interactions to be considered, layer by layer fabrication of biomaterials can be achieved via deposition of film layers on a template based on electrostatic attraction between oppositely charged groups from different polyelectrolytes. Fig. 16 shows the layer by layer fabrication of keratin biomaterials. Using this unique technique, a variety of different polysaccharides and proteins has been converted to the multi-layer structure. At a neutral pH, keratin can act as polyanion and the net charge of the keratin solution can be altered by changing the pH. Hence, it can be used as a polycation as well. Well-known that keratin show high affinity towards Ag-nanoparticles in the polyanion state than that in the polycation state. Using this method, several biomaterials are reported for the potential biomedical

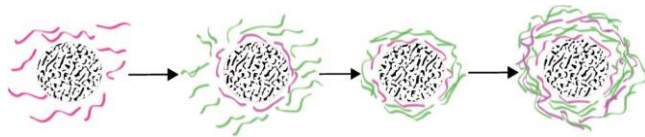


Fig. 16. Layer by layer fabrication of keratin biomaterials.

application. Yang and co-workers^[78] used poly(acrylic acid) (PAA) and the polyelectrolytes, poly(diallyldimethyl ammonium chloride) (PDDA) as positively and negatively charged building blocks to form layers with a controllable thickness. They found that the surface of obtained biomaterials is biocompatible and highly suitable for tissue engineering. The mechanical properties of the obtained biomaterials are also important to confirm the stability of the formed layers.

Hydroxyapatite (HAp) has a hexagonal structure and a stoichiometric Ca/P ratio of 1.67.^[81] The structure and property is similar to the human hard tissues in morphology and composition, particularly, it is closely identical to bone apatite. In addition, the HAp is more stable under physiological conditions as temperature, pH and composition of the body fluids.^[82] Kim et al.,^[83] coated HAp on the ionic cellulose nanofibers for bone regeneration applications. Prior to the coating, the cellulose nanofibers surface was modified with negatively charged group for the better interaction and binding of HAp with the cellulose nanofibers surface. Likewise, keratin is also used for the coating of HAp for tissue engineering. Fig. 17 shows the schematic for the preparation of Keratin-based calcium phosphate biomaterials. Tachibana et al.^[84] prepared keratin sponge with addition of hydroxyapatite. They found that the keratin sponge/HAp composite showed better results in tissue engineering applications. HAp can be coated with keratin sponge by either precipitation method or simply by trapping HA particles inside the keratin sponge matrix. Both composites positively affected and altered the differentiation pattern of the osteoblast cells. However, it was found that the trapped sponges has better results than the precipitated sponges. Alike, Li et al.,^[85] prepared keratin sponge/HAp with 70% of HAp by co-precipitation method showed better viability. The same group prepared two different keratin composites with high contents of HA (40wt %). The two methods are compression moulding technique using 345 MPa pressure and an ice crystal/lyophilisation technique. The prepared two different keratin scaffolds were implanted in the long bones of sheep for 18 weeks. The results showed that the biomaterial has good bone healing property and control, however, the mechanism was not clear. It was doubted that whether the healing property may be related to the incorporation of the keratin or the porosity of the structure. In fact, the porosity of the materials is very crucial for biomedical application. In fact, it can play an important role in blood circulation, cell differentiation, filtration, attachment, and delivery of the body fluid and nutrients to the cell. Later, Katoh et al.^[86] used a compression moulding assisted salt leaching technique. The resultant biomaterial had 90% porosity with pore size of <100, 100–300 and 300–500 μm . Although the results are promising, reason for the mechanical is not clearly explained. There is a continuous search for the alternate process. It is believed that the method using mercaptoethanol by Yamauchi et al.^[87], may be an interesting topic for future research.

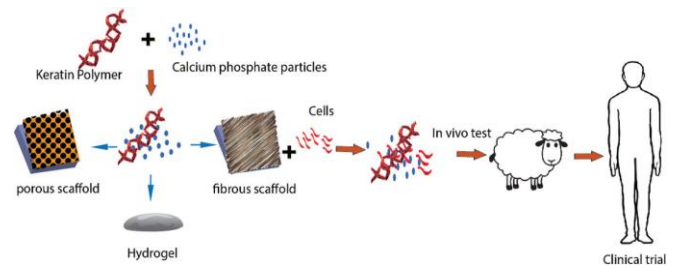


Fig. 17. Keratin-based calcium phosphate biomaterials.^[84]

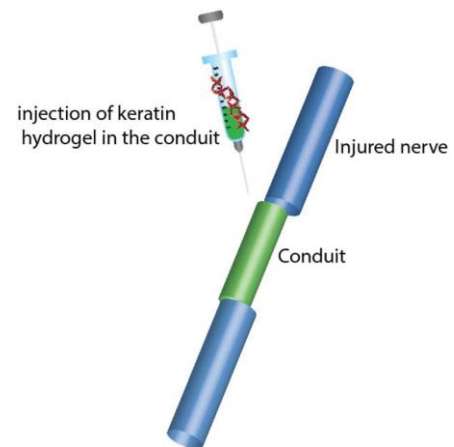


Fig. 18. Nerve regeneration via keratin hydrogel injection into the conduits placed in the defective nerve segment.^[92]

In clinical field, peripheral nerve defects are the most challenging one.^[88,89] In recent year, end to end repair, tubular conduits, and autologous grafts are some of the very useful treatments. For this purpose, protein or polysaccharide biomaterials such as fibrin, collagen, chitosan and hyaluronic acid are often used.^[90,91] The biomaterials mainly used as biomaterial fillers which can provide physical support for the regeneration of cells. It was demonstrated that keratin hydrogel can improve the activity, attachment and proliferation of the nerve Schwann cells via a chemotactic mechanism. Lin et al.,^[92] designed glial cell line-derived neurotrophic factor (GDNF) loaded polycaprolactone based conduit filled with the keratin hydrogel. The biomaterial has capable of repairing 15 mm sciatic nerve injury in the rat model. The results showed that the obtained biomaterial has optimal mechanical and degeneration properties. Hence, the biomaterial is ideal and favors Schwann cell and axon migration, proliferation and consequently nerve repair. Fig. 18 shows the nerve regeneration via keratin hydrogel injection into the conduits placed in the defective nerve segment. Table 3 presented keratin-based films with biomedical applications.^[93-96]

4.4. Agriculture and Textile applications

Keratin is insoluble and difficult to digest by humans and animals. Degradation of this protein is also difficult. The stability of the keratin is mainly based on the packing of the protein chain α -helix (α -keratin) and β -sheet (β -keratin) structures and their linkage by cystine bridges due to high degree of cross-linkage by disulfide bonds, hydrogen bonding and hydrophobic interactions.^[25,46,47] However, microorganisms such as saprophytic and parasitic fungi, a few actinomyces and Bacillus species have ability to degrade the keratin. Recent days, semi slow-released fertilizers are played an important

Table 3. Keratin-based films with biomedical applications

Composition	Ratios	Process conditions	Properties	Ref.
Keratin–chitosan 2 : 1 (w/w)	200 mg of chitosan 15 ml of 75% acetic acid 10 ml of keratin solution (containing 420 mg keratin)	Frozen at –80 °C, slow degradation and antibacterial properties	Max. load (N) 6.30 ± 0.12 Max. extension (mm) 5.12 ± 0.15 Elongation break (%) 21.63 ± 0.13	93
Keratin–gelatin (KG) 2 : 1 (w/w)	200 mg of gelatin 10 ml water, 10 ml of keratin solution (containing 420 mg keratin) 10 ml of gelatin solution (containing 210 mg gelatin)	Frozen at –80 °C, Rapid degradation of gelatin in KG, pores: 20–100 µm	Max. load (N) 7.15 ± 0.18 Max. extension (mm) 6.12 ± 0.12	94
Keratin hydrogel	15% keratin hydrogel	Nerve regeneration	Tenacity – 13.5 cN/tex, elongation – 33%, wetting angle – 33° and, in comparison to pure chitosan fibers, were less prone to biodegradation Neuromuscular recovery with keratin was greater than with empty conduits in most outcome measures	95
Keratin sponge scaffold	The keratin solution (200 µl) containing 8 mg of protein was added to a flat-bottom tube	Frozen -20 °C	Pore size was 100 µm	86
Keratin/poly (vinyl alcohol) composite	10%	Cross linked with glyoxal 10%	Keratin/PVA NFs Young's modulus: 272.8 MPa Tensile strength: 19 MPa, strain: 175.6%	96

role in organic framings. The traditionally available fertilizers are highly limited due to its high cost. Adetunji et al.,^[97] prepared keratin-based organic fertilizer from microbial hydrolysis of feathers for the organic forming. They found that the feather-keratin is cheap, readily available and environmentally friendly offers a promising prospect in agriculture. Similarly, many researchers used feather-keratin to prepare biofertilizers.^[98-100] The advantage of the keratin is the presence of high-N content (15% nitrogen), but the cystine linkages in the keratin structure make it difficult to degrade.^[101] However, there several studies involved the improvement of keratin degradation. Keratin nanoparticles prepared from strong hydrolysis has better degradation ability than that of bulk keratin. So far, the keratin-based biofertilizers has been applied for the growth of banana plants and rye grass cultivation. The continuous research on this topic would come up with most exciting results in the future.

In textile applications, the keratin has played limited role. The stability of the keratin is key factor for the use in textile. Halamine-charged wool cloth exhibited rapid and potent bactericidal activity against several species of bacteria and induced up to a 5.3 log (i.e., 99.9995%) reduction in the colony forming units of *Bacillus thuringiensis* spores within 10 min. Regenerated cellulose/keratin materials chlorinated to display halamines were also effective in killing *Escherichia coli* and *Staphylococcus aureus* bacteria. Some research groups use keratin/cellulose nanofibers as face mask. Keratin-based textile fibers are used as antibacterial cloths.^[101]

5. Conclusions

This review deeply discussed the production methods of keratin from various sources such as hair, fingernails, shells, horn, hooves, toenails, beaks, feathers and claws. The preparation methods and characterization of various nano-composites materials based on carbon, metal/metal-oxide and polymers are discussed well. The potential applications of the keratin-based materials in biomedical, catalysis, textiles, energy and agriculture are discussed in details.

Conflicts of Interest

The authors declare no conflict of interest.

References

- Zhang Z.; Ortiz O.; Goyal R.; Kohn J. *Biodegradable Polymers. Handbook of Polymer Applications in Medicine and Medical Devices.* William Andrew Publishing, 2014, 303-335. [[CrossRef](#)]
- Wang B.; Yang W.; McKittrick J.; Meyers M.A. Keratin: Structure, Mechanical Properties, Occurrence in Biological Organisms, and Efforts at Bioinspiration. *Prog. Mater. Sci.*, 2016, **76**, 229-318. [[CrossRef](#)]
- Fraser R.D.B.; MacRae T.P.; Parry D.A.D.; Suzuki E. The Structure of β -Keratin. *Polymer*, 1969, **10**, 810-826. [[CrossRef](#)]

- 4 Chou C.C.; Buehler M.J. Structure and Mechanical Properties of Human Trichocyte Keratin Intermediate Filament Protein. *Biomacromolecules*, 2012, **13**, 3522-3532. [[CrossRef](#)]
- 5 Fraser R.B.; Parry D.A. The Structural Basis of the Filament-Matrix Texture in the Avian/Reptilian Group of Hard β -Keratins. *J. Struct. Biol.*, 2011, **173**, 391-405. [[CrossRef](#)]
- 6 Trim M.W.; Horstemeyer M.F.; Rhee H.; El Kadiri H.; Williams L.N.; Liao J.; Walters K.B.; McKittrick J.; Park S.J. The Effects of Water and Microstructure on the Mechanical Properties of Bighorn Sheep (*Ovis Canadensis*) Horn Keratin. *Acta Biomater.*, 2011, **7**, 1228-1240. [[CrossRef](#)]
- 7 Taylor A.M.; Bonser R.H.C.; Farrent J.W. The Influence of Hydration on the Tensile and Compressive Properties of Avian Keratinous Tissues. *J. Mater. Sci.*, 2004, **39**, 939-942. [[CrossRef](#)]
- 8 Seki Y.; Schneider M.S.; Meyers M.A. Structure and Mechanical Behavior of a Toucan Beak. *Acta Mater.*, 2005, **53**, 5281-5296. [[CrossRef](#)]
- 9 Lee H.; Noh K.; Lee S.C.; Kwon I.K.; Han D.W.; Lee I.S.; Hwang Y.S. Human Hair Keratin and its-based Biomaterials for Biomedical Applications. *Tissue Eng. Regen. Med.*, 2014, **11**, 255-265. [[CrossRef](#)]
- 10 Haveli S.D.; Walter P.; Patriarche G.; Ayache J.; Castaing J.; Van Elslande E.; Tsoucaris G.; Wang P.A.; Kagan H.B. Hair Fiber as a Nanoreactor in Controlled Synthesis of Fluorescent Gold Nanoparticles. *Nano Lett.*, 2012, **12**, 6212-6217. [[CrossRef](#)]
- 11 Walter P.; Welcomme E.; Hallégot P.; Zaluzec N.J.; Deeb C.; Castaing J.; Veyssi re P.; Br niaux R.; L v que J.L.; Tsoucaris G. Early Use of PbS Nanotechnology for an Ancient Hair Dyeing Formula. *Nano Lett.*, 2006, **6**, 2215-2219. [[CrossRef](#)]
- 12 Deng D.; Gopiraman M.; Kim S.H.; Chung I.M.; Kim I.S. Human Hair: A Suitable Platform for Catalytic Nanoparticles. *ACS Sustainable Chem. Eng.*, 2016, **4**, 5409-5414. [[CrossRef](#)]
- 13 Shavandi A.; Silva T.H.; Bekhit A.A.; Bekhit A.E.D.A. Keratin: Dissolution, Extraction and Biomedical Application. *Biomater. Sci.*, 2017, **5**, 1699-1735. [[CrossRef](#)]
- 14 Singaravelu S.; Ramanathan G.; Raja M.D.; Barge S.; Sivagnanam U.T. Preparation and Characterization of Keratin-Based Biosheet from Bovine Horn Waste as Wound Dressing Material. *Mater. Lett.*, 2015, **152**, 90-93. [[CrossRef](#)]
- 15 Harrap B.S.; Gillespie J.M. A Further Study on the Extraction of Reduced Proteins from Wool. *Aust. J. Biol. Sci.*, 1963, **16**, 542-556. [[CrossRef](#)]
- 16 Gillespie J.M. The Isolation and Properties of Some Soluble Proteins from Wool VIII. The Proteins of Copper-Deficient Wool. *Aust. J. Biol. Sci.*, 1964, **17**, 282-300. [[CrossRef](#)]
- 17 Kitahara T.; Ogawa H. The Extraction and Characterization of Human Nail Keratin. *J. Dermatol. Sci.*, 1991, **2**, 402-406. [[CrossRef](#)]
- 18 Schrooyen P.M.; Dijkstra P.J.; Oberth r R.C.; Bantjes A.; Feijen J. Partially Carboxymethylated Feather Keratins. 1. Properties in Aqueous Systems. *J. Agric. Food Chem.*, 2000, **48**, 4326-4334. [[CrossRef](#)]
- 19 Goddard D.R.; Michaelis L. Derivatives of Keratin. *J. Biol. Chem.*, 1935, **112**, 361-371. [[CrossRef](#)]
- 20 W. E. Savage. The Dispersion of Wool Protein by Thiols in Acid Solution. *Text. Res. J.*, 1960, **30**, 1-10 [[CrossRef](#)]
- 21 Kitahara T.; Ogawa H. The Extraction and Characterization of Human Nail Keratin. *J. Dermatol. Sci.*, 1991, **2**, 402-406. [[CrossRef](#)]
- 22 Yamauchi K.; Yamauchi A.; Kusunoki T.; Kohda A.; Konishi Y. Preparation of Stable Aqueous Solution of Keratins, and Physicochemical and Biodegradational Properties of Films. *Journal of Biomedical Materials Research: An Official Journal of the Society for Biomaterials and The Japanese Society for Biomaterials*, 1996, **31**, 439-444. [[CrossRef](#)]
- 23 Nakamura A.; Arimoto M.; Takeuchi K.; Fujii T. A Rapid Extraction Procedure of Human Hair Proteins and Identification of Phosphorylated Species. *Biol. Pharm. Bull.*, 2002, **25**, 569-572. [[CrossRef](#)]
- 24 Kakkar P.; Madhan B.; Shanmugam G. Extraction and Characterization of Keratin from Bovine Hoof: A Potential Material for Biomedical Applications. *SpringerPlus*, 2014, **3**, 596. [[CrossRef](#)]
- 25 Gopiraman M.; Saravanamoorthy S.; Chung I.M. Highly Active Human-Hair-Supported Noble Metal (Ag or Ru) Nanocomposites for Rapid and Selective Reduction of P-Nitrophenol to P-Aminophenol. *Res. Chem. Intermed.*, 2017, **43**, 5601-5614. [[CrossRef](#)]
- 26 Gopiraman M.; Chung I.M. Multifunctional Human-Hair Nanocomposites for Oxidation of Alcohols, Aza-Michael Reactions and Reduction of 2-Nitrophenol. *Korean J. Chem. Eng.*, 2017, **34**, 2169-2179. [[CrossRef](#)]
- 27 Gopiraman M.; Deng D.; Zhang K.Q.; Kai W.; Chung I.M.; Karvemu R.; Kim I.S. Utilization of Human Hair as a Synergistic Support for Ag, Au, Cu, Ni, and Ru Nanoparticles: Application in Catalysis. *Ind. Eng. Chem. Res.*, 2017, **56**, 1926-1939. [[CrossRef](#)]
- 28 Xu H.; Shi Z.; Reddy N.; Yang Y. Intrinsically Water-Stable Keratin Nanoparticles and their In Vivo Biodistribution for Targeted Delivery. *J. Agri. Food Chem.*, 2014, **62**, 9145-9150. [[CrossRef](#)]
- 29 Thakur V.K.; Thakur M.K. eds., Chemical Functionalization of Carbon Nanomaterials: Chemistry and Applications. CRC Press, 2015, [[CrossRef](#)]
- 30 Chng L.L.; Erathodiyil N.; Ying J.Y. Nanostructured Catalysts for Organic Transformations. *Acc. Chem. Res.*, 2013, **46**, 1825-1837. [[CrossRef](#)]
- 31 Komarneni S. Nanocomposites. *J. Mater. Chem.*, 1992, **2**, 1219-1230. [[CrossRef](#)]
- 32 Gopiraman M.; Muneeswaran M.; Kim I.S. Highly Porous Ru/C and Cu/C Nanocatalysts Derived from Custard Apple for Rapid and Selective Reduction of P-Nitrophenol. *Nano Prog.*, 2019, **1**, 30-36. [[CrossRef](#)]
- 33 Selvamani A.; Babu C.M.; Ramkumar V.; Sundaravel B. Reduced Graphene Oxide Decorated Au Nanoparticles as an Efficient Electrode for the Determination of Hydroquinone. *Nano Prog.*, 2019, **1**, 10-15. [[CrossRef](#)]
- 34 Gopiraman M.; Ganesh Babu S.; Khatri Z.; Kai W.; Kim Y.A.; Endo M.; Karvemu R.; Kim I.S. Dry Synthesis of Easily Tunable Nano Ruthenium Supported on Graphene: Novel Nanocatalysts for Aerial Oxidation of Alcohols and Transfer Hydrogenation of Ketones. *J. Phys. Chem. C*, 2013, **117**, 23582-23596. [[CrossRef](#)]
- 35 Gopiraman M.; Karvemu R.; Kim I.S. Highly Active, Selective, and Reusable RuO₂/SWCNT Catalyst for Heck Olefination of Aryl Halides. *ACS Catal.*, 2014, **4**, 2118-2129. [[CrossRef](#)]
- 36 Gopiraman M.; Saravanamoorthy S.; Ullah S.; Ilangovan A.; Kim I.S.; Chung I.M. Reducing-Agent-Free Facile Preparation of Rh-Nanoparticles Uniformly Anchored on Onion-Like Fullerene for Catalytic Applications. *RSC Adv.*, 2020, **10**, 2545-2559. [[CrossRef](#)]
- 37 Saravanamoorthy S.; Vijayakumar E.; Jemimah S.; Ilangovan A. Catalytic Reduction of P-Nitrophenol and Carbonyl Compounds by NiO-Nanoparticles Fastened Graphene Oxide. *Chem. Sci. Eng. Res.*, 2019, **1**, 1-7. [[CrossRef](#)]
- 38 Ashok K.V.; Aswathy T.V.; Raja T. Exploring the Influence of Transition Metal Incorporation on the Performance of Cerium Vanadates in 1-Butene Oxidative Dehydrogenation. *Nano Prog.*, 2019, **1**, 22-29. [[CrossRef](#)]
- 39 Lu X.; Zhang W.; Wang C.; Wen T.C.; Wei Y. One-Dimensional Conducting Polymer Nanocomposites: Synthesis, Properties and Applications. *Prog. Polym. Sci.*, 2011, **36**, 671-712. [[CrossRef](#)]
- 40 Jerome P.; Arafath S.Y.; Babu S.G. Controlled Green Synthesis of Polymer Functionalized Zinc Oxide Nanoparticles. *Green Rep.*, 2020, **1**, 16-20. [[CrossRef](#)]
- 41 Kalia S.; Kango S.; Kumar A.; Haldorai Y.; Kumari B.; Kumar R. Magnetic Polymer Nanocomposites for Environmental and Biomedical Applications. *Colloid Polym. Sci.*, 2014, **292**, 2025-2052. [[CrossRef](#)]
- 42 Babu C.M.; Balasubramanian R.; Vinodh R.; Thirukumaran P.; Shakila Parveen A.; Selvamani A.; Sundaravel B.; Ramkumar V. Cost-Effective Alumina-Polymer Nanocomposite: An Excellent Candidate for the Removal of Heavy Metal Ions from Environmental Samples. *Nano Prog.*, 2019, **1**, 1-9. [[CrossRef](#)]
- 43 Li J.S.; Li Y.; Liu X.; Zhang J.; Zhang Y. Strategy To Introduce An Hydroxyapatite-Keratin Nanocomposite into a Fibrous Membrane for Bone Tissue Engineering. *J. Mater. Chem. B*, 2013, **1**, 432-437. [[CrossRef](#)]
- 44 Fujimori K.; Gopiraman M.; Kim H.K.; Kim B.S.; Kim I.S. Mechanical and Electromagnetic Interference Shielding Properties of Poly (Vinyl Alcohol)/Graphene and Poly (Vinyl Alcohol)/Multi-Walled Carbon

- Nanotube Composite Nanofiber Mats and the Effect of Cu Top-Layer Coating. *J. Nanosci. Nanotechnol.*, 2013, **13**, 1759-1764. [[CrossRef](#)]
- 45 Rodríguez-González C.; Kharissova O.V.; Martínez-Hernández A.N.A.L.; Castaño V.M.; Velasco-Santos C. Graphene Oxide Sheets Covalently Grafted with Keratin Obtained from Chicken Feathers. *Digest J. Nanomater. Biostruct.*, 2013, **8**, 127-38. [[CrossRef](#)]
- 46 Zhou Y.; Zeng H.C. Alumina-Supported Metal Catalysts inside a Mesoporous Aluminum-Silicate Shell: Nanoscale Reactors Prepared through the Transformation of MIL-96 (Al) Nanocrystals. *Chem. Cat. Chem.*, 2016, **8**, 1283-1287. [[CrossRef](#)]
- 47 Tao F.F. Synthesis, Catalysis, Surface Chemistry and Structure of Bimetallic Nanocatalysts. *Chem. Soc. Rev.*, 2012, **41**, 7977-7979. [[CrossRef](#)]
- 48 Mielby J.; Poreddy R.; Engelbrekt C.; Kegaes S. Highly Selective formation of Imines Catalyzed by Silver Nanoparticles Supported on Alumina. *Chin. J. Catal.*, 2014, **35**, 670. [[CrossRef](#)]
- 49 Chen G.; Gao W.; Wang X.; Huo H.; Li W.; Zhang L.; Li R.; Li Z. Magnetic NiO Nanoparticles Confined within Open Ends MWCNTs: A Novel and Highly Active Catalyst for Hydrogenation and Synthesis of Imines. *RSC Adv.*, 2016, **6**, 58805. [[CrossRef](#)]
- 50 Chung I.M.; Gopiraman M. Heteroatom-Rich Hierarchically Porous Carbon Nanosheets Derived from Human Hair as an Efficient Metal-Free Catalyst for Imine Formation. *React. Kinet., Mech. Cat.*, 2017, **122**, 205-215. [[CrossRef](#)]
- 51 Wu K.; Wei X.; Zhou X.; Wu D.; Liu X.; Ye Y.; Wang Q. NiCo₂ Alloys: Controllable Synthesis, Magnetic Properties, and Catalytic Applications in Reduction of 4-Nitrophenol. *J. Phys. Chem. C*, 2011, **115**, 16268-16274. [[CrossRef](#)]
- 52 Zhao P.X.; Feng X.W.; Huang D.S.; Yang G.Y.; Astruc D. Basic Concepts and Recent Advances in Nitrophenol Reduction by Gold-and other Transition Metal Nanoparticles. *Coordin. Chem. Rev.*, 2015, **287**, 114-136. [[CrossRef](#)]
- 53 Narayanan K.B.; Sakthivel N. Heterogeneous Catalytic Reduction of Anthropogenic Pollutant, 4-Nitrophenol by Silver-Bionanocomposite using *Cylindrocladium Floridanum*. *Bioresour. Technol.*, 2011, **102**, 10737-10740. [[CrossRef](#)]
- 54 Meng N.; Cheng J.; Zhou Y.; Nie W.; Chen P. Green Synthesis of Layered 1T-MoS₂/Reduced Graphene Oxide Nanocomposite with Excellent Catalytic Performances for 4-Nitrophenol Reduction. *Appl. Surf. Sci.*, 2017, **396**, 310-318. [[CrossRef](#)]
- 55 Ji T.; Chen L.; Schmitz M.; Bao F.S.; Zhu J. Hierarchical Macrotube/Mesopore Carbon Decorated with Mono-Dispersed Ag Nanoparticles as a Highly Active Catalyst. *Green Chem.*, 2015, **17**, 2515-2523. [[CrossRef](#)]
- 56 Hareesh K.; Joshi R.P.; Sunitha D.V.; Bhoraskar V.N.; Dhole S.D. Anchoring of Ag-Au Alloy Nanoparticles on Reduced Graphene Oxide Sheets for the Reduction of 4-Nitrophenol. *Appl. Surf. Sci.*, 2016, **389**, 1050-1055. [[CrossRef](#)]
- 57 Sahoo A.; Tripathy S. K.; Dehury N.; Patra S. A Porous Trimetallic Au@Pd@Ru Nanoparticle System: Synthesis, Characterisation and Efficient Dye Degradation and Removal. *J. Mater. Chem. A*, 2015, **3**, 19376-19383. [[CrossRef](#)]
- 58 Tang J.; Tang D.; Su B.; Huang J.; Qiu B.; Chen G. Enzyme-Free Electrochemical Immunoassay with Catalytic Reduction of p-Nitrophenol and Recycling of p-Aminophenol using Gold Nanoparticles-Coated Carbon Nanotubes as Nanocatalysts. *Biosens. Bioelectron.*, 2011, **26**, 3219-3226. [[CrossRef](#)]
- 59 Pozun Z.D.; Rodenbusch S.E.; Keller E.; Tran K.; Tang W.; Stevenson K.J.; Henkelman G. A Systematic Investigation of p-Nitrophenol Reduction by Bimetallic Dendrimer Encapsulated Nanoparticles. *J. Phys. Chem. C*, 2013, **117**, 7598-7604. [[CrossRef](#)]
- 60 Yang Y.; Ren Y.; Sun C.; Hao S. Facile Route Fabrication of Nickel based Mesoporous Carbons with High Catalytic Performance towards 4-Nitrophenol Reduction. *Green Chem.*, 2014, **16**, 2273-2280. [[CrossRef](#)]
- 61 Wang X.; Zhao Z.; Ou D.; Tu B.; Cui D.; Wei X.; Cheng M. Highly Active Ag Clusters Stabilized on TiO₂ Nanocrystals for Catalytic Reduction of p-Nitrophenol. *Appl. Surf. Sci.*, 2016, **385**, 445-452. [[CrossRef](#)]
- 62 Antonels N.C.; Meijboom R. Preparation of Well-Defined Dendrimer Encapsulated Ruthenium Nanoparticles and their Evaluation in the Reduction of 4-Nitrophenol According to the Langmuir-Hinshelwood Approach. *Langmuir*, 2013, **29**, 13433-13442. [[CrossRef](#)]
- 63 Goksu H.; Ho S.F.; Metin O.; Korkmaz K.; Garcia A.M.; Gultekin M.S.; Sun S. Tandem Dehydrogenation of Ammonia Borane and Hydrogenation of Nitro/Nitrile Compounds Catalyzed by Graphene-Supported NiPd Alloy Nanoparticles. *ACS Catal.*, 2014, **4**, 1777-1782. [[CrossRef](#)]
- 64 Kuroda K.; Ishida T.; Haruta M. Reduction of 4-Nitrophenol to 4-Aminophenol over Au Nanoparticles Deposited on PMMA. *J. Mol. Catal. A: Chem.*, 2009, **298**, 7-11. [[CrossRef](#)]
- 65 Dong Z.; Le X.; Dong C.; Zhang W.; Li X.; Ma J. Ni@Pd Core-Shell Nanoparticles Modified Fibrous Silica Nanospheres as Highly Efficient and Recoverable Catalyst for Reduction of 4-Nitrophenol and Hydrodechlorination of 4-Chlorophenol. *Appl. Catal. B-Environ.*, 2015, **162**, 372-380. [[CrossRef](#)]
- 66 Tian Y.; Liu Y.; Pang F.; Wang F.; Zhang X. Green Synthesis of Nanostructured Ni-Reduced Graphene Oxide Hybrids and their Application for Catalytic Reduction of 4-Nitrophenol. *Colloids Surf., A Physicochem. Eng. Asp.*, 2015, **464**, 96-103. [[CrossRef](#)]
- 67 Nasrollahzadeh M.; Atarod M.; Sajadi S.M. Green Synthesis of the Cu/Fe₃O₄ Nanoparticles using Morindamorindoides Leaf Aqueous Extract: A Highly Efficient Magnetically Separable Catalyst for the Reduction of Organic Dyes in Aqueous Medium at Room Temperature. *Appl. Surf. Sci.*, 2016, **364**, 636-644. [[CrossRef](#)]
- 68 Lv J.J.; Wang A.J.; Ma X.; Xiang R.Y.; Chen J.R.; Feng J.J. One-Pot Synthesis of Porous Pt-Au Nanodendrites Supported on Reduced Graphene Oxide Nanosheets toward Catalytic Reduction of 4-Nitrophenol. *J. Mater. Chem. A*, 2015, **3**, 290-296. [[CrossRef](#)]
- 69 Ramesh P.; Prabhakarn A.; Shankar A.; Jagatheesan R.; Sambathkumar S.; Jebasingh B.; Vasanthkumar S. Covalent Grafting of N-Containing Compound with Graphene Oxide: Efficient Electrode Material for Supercapacitor. *Chem. Sci. Eng. Res.*, 2019, **1**, 8-15. [[CrossRef](#)]
- 70 Vangari M.; Pryor T.; Jiang L. Supercapacitors: Review of Materials and Fabrication Methods. *J. Energ. Eng.*, 2013, **139**, 72-79. [[CrossRef](#)]
- 71 Gopiraman M.; Deng D.; Kim B.S.; Chung I.M.; Kim I.S. Three-Dimensional Cheese-Like Carbon Nanoarchitecture with Tremendous Surface Area and Pore Construction Derived from Corn as Superior Electrode Materials for Supercapacitors. *Appl. Surf. Sci.*, 2017, **409**, 52-59. [[CrossRef](#)]
- 72 Qian W.; Sun F.; Xu Y.; Qiu L.; Liu C.; Wang S.; Yan F. Human Hair-Derived Carbon Flakes for Electrochemical Supercapacitors. *Energy Environ. Sci.*, 2014, **7**, 379-386. [[CrossRef](#)]
- 73 Deng D.; Kim B.S.; Gopiraman M.; Kim I.S. Needle-Like MnO₂/Activated Carbon Nanocomposites Derived from Human Hair as Versatile Electrode Materials for Supercapacitors. *RSC Adv.*, 2015, **5**, 81492-81498. [[CrossRef](#)]
- 74 Shoichet M.S. Polymer Scaffolds for Biomaterials Applications. *Macromolecules*, 2010, **43**, 581-591. [[CrossRef](#)]
- 75 Sangeetha A.; Samyuktha L.; Atya K.; Neha H.; Rakesh K.S.; Shantveer G.U.; Kaiser J. In Vivo Interactions of Nanosized Titania Anatase and Rutile Particles Following Oral Administration. *Nano Prog.*, 2020, **2**, 11-20. [[CrossRef](#)]
- 76 Ha T.L.B.; Quan T.M.; Vu D.N. Naturally Derived Biomaterials: Preparation and Application. *J. Tissue Eng. Regen. Med.* IntechOpen, 2013. [[CrossRef](#)]
- 77 Borges J.; Mano, J.F. Molecular Interactions Driving the Layer-By-Layer Assembly of Multilayers. *Chem. Rev.*, 2014, **114**, 8883-8942. [[CrossRef](#)]
- 78 Yang X.; Zhang H.; Yuan X.; Cui S. Wool Keratin: A Novel Building Block for Layer-By-Layer Self-Assembly. *J. Colloid Interface Sci.*, 2009, **336**, 756-760. [[CrossRef](#)]
- 79 Zhang H.; Yu Y.; Cui S. Multilayer Fluorescent Thin Films based on Keratin-Stabilized Silver Nanoparticles. *Colloids Surf. A*, 2011, **384**, 501-506. [[CrossRef](#)]
- 80 Jin G.; Jiang L.M.; Yi D.M.; Sun H.Z.; Sun H.C. The Influence of Surface Modification on the Photoluminescence of CdTe Quantum Dots: Realization of Bio-Imaging via Cost-Effective Polymer. *Chem. Phys. Chem.*, 2015, **16**, 3687-3694. [[CrossRef](#)]
- 81 Zhou H.; Lee J. Nanoscale Hydroxyapatite Particles for Bone Tissue Engineering. *Acta Biomater.*, 2011, **7**, 2769-2781. [[CrossRef](#)]

- 82 Boccaccini A.R.; Erol M.; Stark W.J.; Mohn D.; Hong Z.; Mano J.F. Polymer/Bioactive Glass Nanocomposites for Biomedical Applications: A Review. *Compos. Sci. Technol.*, 2010, **70**, 1764-1776. [[CrossRef](#)]
- 83 Yamaguchi K.; Prabakaran M.; Ke M.; Gang X.; Chung I.M.; Um I.C.; Gopiraman M.; Kim I.S. Highly Dispersed Nanoscale Hydroxyapatite on Cellulose Nanofibers for Bone Regeneration. *Mater. Lett.*, 2016, **168**, 56-61. [[CrossRef](#)]
- 84 Tachibana A.; Furuta Y.; Takeshima H.; Tanabe T.; Yamauchi K. Fabrication of Wool Keratin Sponge Scaffolds for Long-Term Cell Cultivation. *J. Biotechnol.*, 2002, **93**, 165-170. [[CrossRef](#)]
- 85 Li J.; Liu X.; Zhang J.; Zhang Y.; Han Y.; Hu J.; Li Y. Synthesis and Characterization of Wool Keratin/Hydroxyapatite Nanocomposite. *J. Biomed. Mater. Res. Part B*, 2012, **100**, 896-902. [[CrossRef](#)]
- 86 Katoh K.; Tanabe T.; Yamauchi K. Novel Approach to Fabricate Keratin Sponge Scaffolds with Controlled Pore Size and Porosity. *Biomaterials*, 2004, **25**, 4255-4262. [[CrossRef](#)]
- 87 Yamauchi K.; Yamauchi A.; Kusunoki T.; Kohda A.; Konishi Y. Preparation of Stable Aqueous Solution of Keratins, and Physicochemical and Biodegradational Properties of Films. *J. Biomed. Mater. Res.*, 1996, **31**, 439-444. [[CrossRef](#)]
- 88 Xu H.; Holzwarth J.M.; Yan Y.; Xu P.; Zheng H.; Yin Y.; Li S.; Ma P.X. Conductive PPy/PDLLA Conduit for Peripheral Nerve Regeneration. *Biomaterials*, 2014, **35**, 225-235. [[CrossRef](#)]
- 89 Sierpinski P.; Garrett J.; Ma J.; Apel P.; Klorig D.; Smith T.; Koman L.A.; Atala A.; Van Dyke M. The Use of Keratin Biomaterials Derived from Human Hair for the Promotion of Rapid Regeneration of Peripheral Nerves. *Biomaterials*, 2008, **29**, 118-128. [[CrossRef](#)]
- 90 Guo J.; Pan S.; Yin X.; He Y.F.; Li T.; Wang R.M. pH-Sensitive Keratin-based Polymer Hydrogel and its Controllable Drug-Release Behavior. *J. Appl. Polym. Sci.*, 2015, **132**, 41572. [[CrossRef](#)]
- 91 Labrador R.O.; Buti M.; Navarro X. Influence of Collagen and Laminin Gels Concentration on Nerve Regeneration after Resection and Tube Repair. *Exp. Neurol.*, 1998, **149**, 243-252. [[CrossRef](#)]
- 92 Lin Y.C.; Ramadan M.; Van Dyke M.; Kokai L.E.; Philips B. J.; Rubin J.P.; Marra K. G. Keratin Gel Filler for Peripheral Nerve Repair in a Rodent Sciatic Nerve Injury Model. *Plast. Reconstr. Surg.*, 2012, **129**, 67-78. [[CrossRef](#)]
- 93 Balaji S.; Kumar R.; Sripriya R.; Kakkar P.; Ramesh D.V.; Reddy P.N.K.; Sehgal P.K. Preparation and Comparative Characterization of Keratin-Chitosan and Keratin-Gelatin Composite Scaffolds for Tissue Engineering Applications. *Mater. Sci. Eng. C*, 2012, **32**, 975-982. [[CrossRef](#)]
- 94 Kakkar P.; Verma S.; Manjubala I.; Madhan B. Development of Keratin-Chitosan-Gelatin Composite Scaffold for Soft Tissue Engineering. *Mater. Sci. Eng. C*, 2014, **45**, 343-347. [[CrossRef](#)]
- 95 Apel P.J.; Garrett J.P.; Sierpinski P.; Ma J.; Atala A.; Smith T.L.; Koman L.A.; Van Dyke M.E. Peripheral Nerve Regeneration using a Keratin-based Scaffold: Long-Term Functional and Histological Outcomes in a Mouse Model. *J. Hand Surg. Am.*, 2008, **33**, 1541-1547. [[CrossRef](#)]
- 96 Choi J.; Panthi G.; Liu Y.; Kim J.; Chae S.H.; Lee C.; Park M.; Kim H.Y. Keratin/Poly (Vinyl Alcohol) Blended Nanofibers with High Optical Transmittance. *Polymer*, 2015, **58**, 146-152. [[CrossRef](#)]
- 97 Adetunji C.O.; Makanjuola O.R.; Arowora K.A.; Afolayan S.S.; Adetunji, J.B. Production and Application of Keratin-based Organic Fertilizer from Microbially Hydrolyzed Feathers to Cowpea (*Vigna Unguiculata*). *J. Sci. Eng. Res.*, 2012, **3**, 1-9. [[CrossRef](#)]
- 98 Chikura T.; Izumi N.; Matsumoto S. Manufacture of Amino Acid Containing Fertilizers. Jpn. Kokai Tokkyo Koho, JP 06 40, 1994.
- 99 Reddy N. Non-Food Industrial Applications of Poultry Feathers. *Waste Manage.*, 2015, **45**, 91-107. [[CrossRef](#)]
- 100 Bhavani G.; Kavitha A.; Shrey B.; Sai Shiva Krishna Prasad Vurukonda. Microbial Degradation of Keratin and its Agro Industrial Prospective Applications. *Int. J. Curr. Adv. Res.*, 2018, **7**, 9709-9716. [[CrossRef](#)]
- 101 Dickerson M.B.; Sierra A.A.; Bedford N.M.; Lyon W.J.; Gruner W.E.; Mirau P.A.; Naik R.R. Keratin-based Antimicrobial Textiles, Films, and Nanofibers. *J. Mater. Chem. B*, 2013, **1**, 5505-5514. [[CrossRef](#)]



© 2020, by the authors. Licensee Ariviyal Publishing, India. This article is an open access article distributed under the terms and conditions of the Creative Commons Attribution (CC BY) license (<http://creativecommons.org/licenses/by/4.0/>).